

# Weather Station Integrated with Wireless Sensor Network for Micro Climate Monitoring

Chia-Yen Lee<sup>1\*</sup>, Yu-Hsiang Wang<sup>2</sup>, Rong-Hua Ma<sup>3</sup>

<sup>1</sup>Department of Materials Engineering, National Pingtung University of Science and Technology, Taiwan.

<sup>2</sup>EU Jason Co., Ltd., Taiwan

<sup>3</sup>Department of Mechanical Engineering, Chinese Military Academy

leecy@mail.npust.edu.tw 886-8-770-3202 Ext.7561

In recent years, emerging Micro-Electro-Mechanical Systems (MEMS) technology and micromachining techniques have been a popular approach to the miniaturization of sensors. More importantly, the functionality and reliability of these micro-sensors has been increased considerably by integrating them with mature logic IC technology or other sensors. To effectively gauge the weather, it is essential to gather data, such as temperature, humidity, air pressure, airflow direction and velocity over a wide area. Previous studies have reported on the use of MEMS sensors for monitoring individual weather parameters, such as pressure [1], flow rate [2,3], humidity [4,5], temperature, and multi-parameters (two or more) [6-10].

The current study developed a fabrication process integrating Pt resistor temperature detectors (RTD), Au inter-digitated electrodes (IDEs) and polyimide layers for sensing humidity, Pt-piezoresistor-based pressure sensors, and flow sensors for the identification of airflow direction and velocity. The measurement of temperature was based on variations in linear resistance associated with changes in ambient temperature. The Au IDEs were covered with a water-absorbent polyimide layer to measure humidity, based on changes in the dielectric constant of the water-absorbent polyimide layer associated with changes in ambient moisture. To form the flow sensor and pressure sensor, eight pairs of heating and sensing resistors and four piezoresistors were manufactured on a membrane structure released after a back-etching process. The direction of airflow was determined according to fluctuations in the resistance of the sensors caused by air flowing through the sensor in a specific direction. The velocity of the airflow could then be obtained by summing the total variations measured by the sensing resistors. Finally, the electrical signals produced by temperature, humidity, pressure, airflow velocity and changes in direction were amplified and converted into voltage signals using an analogy circuit, connected between the MEMS-based sensors and the Octopus II sensor node. Finally, the Octopus II sensor node converted the analog signals into digital signals and transmitted them wirelessly into a data logger or a computer, as shown in Figure 1.

The sensor array of the proposed MEMS-based weather monitoring system was fabricated on a silicon nitride film over a silicon wafer utilizing platinum resistors as heating and sensing devices. Figure 2 illustrates the configuration and dimensions of the sensor array developed in the study.

In Figure 2(a), the developed sensors comprise a Pt RTD, a humidity sensor with Au IDEs, a Pt-piezoresistor-based pressure sensor, and a flow sensor to determine the direction and velocity of airflow integrated onto a single chip. Note that Au was used for the bonding pads to connect the sensors to the circuits.

As shown in Figure 2(b), the Au bonding pads were deposited on the two edges of the Pt RTD. The size of the resistor used for the Pt RTD was  $1,800 \mu\text{m} \times 300 \mu\text{m}$  (length  $\times$  width). Temperature measurements were based on linear variations in electrical resistance associated with changes in ambient temperature. Figure 2(c) shows the configuration of the humidity sensor, comprising a vapor absorbent film of polyimide (PW-1500, Toray Industries, Inc.) and coplanar Au IDEs. The piezoresistors used in the pressure sensor [Figure 2(c)] and the resistors utilized in the flow sensor [Figure 2(d)] were deposited over silicon nitride membranes of the same dimensions ( $3,000 \mu\text{m} \times 3,000 \mu\text{m}$ ),

were released by a back-etching process to form a heat insulating membrane over the thermal flow sensor. This was sealed with a back plate to obtain a vacuum cavity to house the pressure sensor. In Figure 2(e), the flow sensor is used to

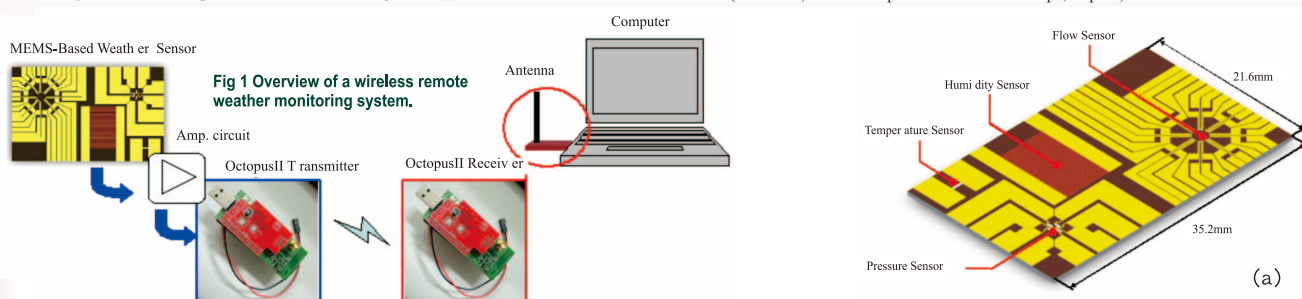
determine the direction and velocity of airflow using eight pairs of heating and sensing resistors on a membrane structure. The dimensions of the heaters and detectors are  $100 \mu\text{m} \times 100 \mu\text{m}$  and  $400 \mu\text{m} \times 100 \mu\text{m}$ , respectively.

As an electrical charge is applied to the heating resistors, the measurement of the direction of flow is based on the difference in relative output of the eight sensing resistors in response to variations in the temperature induced by the airflow due to the Joule effect. As the air passes over each pair of resistors in a particular direction, signal variations occur between pairs of resistors resulting in measurable changes in the resistance. Through manipulation and evaluation of the signals obtained from all of the sensing resistors, both the direction of flow and flow rate can be reliably determined.

In this study, a WSN platform device (Octopus II-A) was used to perform analog/digital conversion and wireless transmission. This is an open-source visualization and control tool for sensor networks developed in the TinyOS environment (TinyOS is an open-source operating system designed for low-power wireless devices, such as sensor networks, ubiquitous computing, personal area networks, smart buildings and smart meters). The MSP430F611 core processing chip in Octopus II was produced by Texas Instruments, Inc., and the Chipcon CC2420 chip was used for wireless communication according to the IEEE 802.15.4 specification.

In this study, Pt resistors were used as piezoresistors, heating and sensing resistors were used to measure deformations in the membrane and temperature, and Au was used as the bonding pads and lead wires connecting the external analog circuits. The low resistivity of Au reduced the resistance of the leads. Figure 3 shows the process of fabricating the sensor array of the MEMS-based weather monitoring system. Initially, a  $1.0 \mu\text{m}$  low-stress nitride layer was deposited on both sides of a single-side polished silicon wafer. Before depositing the Pt, a thin layer of Cr ( $0.02 \mu\text{m}$ ) was deposited as an adhesion layer. An electron beam evaporation process was then used to deposit a  $0.1 \mu\text{m}$  layer of Pt. The same technique was used to add a layer of Au ( $0.4 \mu\text{m}$ ) to serve as an electrode and to provide electrical leads. To form the structure of the membrane, a back-etching nitride mask was patterned using an SF<sub>6</sub> RIE plasma released in a KOH etchant (40 wt%, 85°C, from J. T. Baker). A layer of polyimide (PW-1500, Toray Industries, Inc.) was then spun on and patterned as a moisture sensing layer ( $15 \mu\text{m}$  thick after curing) to play the role of humidity sensor. Finally, a layer of UV adhesive (OPAS-101, OPAS UV curing corp., Taiwan) was spun on a glass back plate and bonded with the chip of the sensor array in a negative pressure chamber to obtain a vacuum-sealed cavity for the following air pressure measurement.

This study conducted a systematic investigation of the performance of the fabricated sensor array of the MEMS-based weather monitoring system (Figure 4). The characteristic effects of temperature, humidity, and pressure sensors were carried out in a climate chamber (HRM-80FA, Terchy, Taiwan) setup in a vacuum chamber. The climate chamber was capable of providing a humidity range of 30% RH–95% RH and a temperature range of 20–85°C. The temperature and humidity in the climate chamber could be adjusted separately and maintained at constant levels. For reference purposes, the humidity and temperature was also measured using a reference humidity/temperature meter (HT-3009, Lutron Electronics, Inc., Taiwan). Pressure measurements were carried out using a vacuum pump and an air compressor to vary the air pressure within the chamber. A reference pressure meter (PG-100, Nidec Copal Electronics Corp., Japan) was used to measure the actual



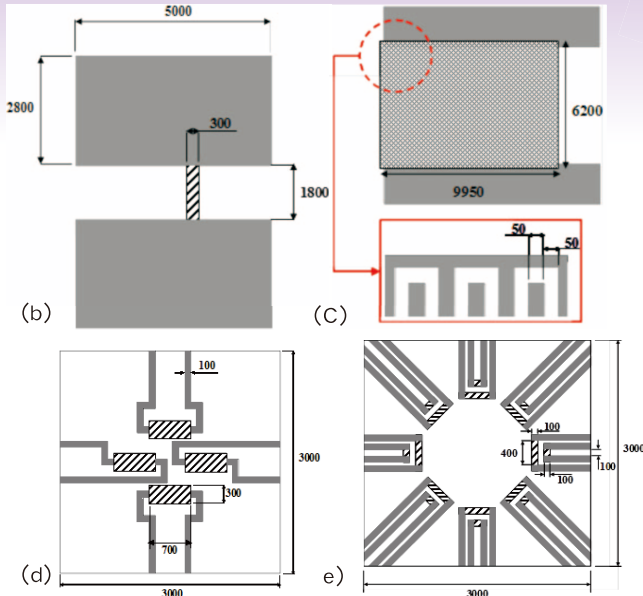


Figure 2. Configuration and dimensions of integrated sensor array of MEMS-based weather monitoring system: (a) overview, (b) RTD, (c) humidity sensor, (d) pressure sensor and (e) flow sensor. (unit:  $\mu\text{m}$ )

pressure value to calibrate the response of the sensor. The flow sensor was tested in a wind tunnel in which the sensor was placed on a rotary table (LCPR60, Tan Lian E-O Co., Ltd., Taiwan). Airflow between 0 to  $8\text{ ms}^{-1}$  was used to evaluate the signal response of the sensing resistors located at eight different points within the membrane. Note that for reference purposes the air flow rate was also measured using a reference anemometer (AM-4203, Lutron Electronics, Inc, Taiwan).

The electrical signals associated with temperature, humidity, pressure, airflow velocity and changes in direction were amplified and converted into signals of a specific voltage using an analog circuit, connected between the sensor array and the Octopus II sensor node. Through the Octopus II sensor node, the analog voltage signals were converted into digital signals and transmitted wirelessly to the data logger.

Figures 5 and 6 show the signal conversion and determination path of the signals from the sensor array. The resistance values of the eight flow sensors were obtained from the resistors located at eight points on the membrane, and the rate of airflow was obtained by evaluating the sum of the total variations between sensing resistors as the airflow passed over the flow sensor. The resistance signals could then be amplified and converted into voltage signals using Wheatstone bridge circuits. After the ADC operation of a  $\mu$ -controller and the Octopus II-A, the digital signals were sent to the Octopus II-A receiver for the following data operation.

This study proposed a wireless remote weather monitoring system based on MEMS and WSN technology for monitoring temperature, humidity, pressure, flow rate and direction. The proposed sensor array used in the wireless remote weather monitoring system comprised a Pt RTD, a capacitive humidity sensor, a piezoresistive pressure sensor, and anemometers integrated through bulk-micromachining technology. The sensing signals were transmitted and received between the Octopus II-A sensor nodes using WSN Technology, after which the signal was amplified and the ADC of the original signals was processed. The experimental results show the response of the temperature sensor increases linearly with the ambient temperature. Its average TCR value was  $8.2 \times 10^{-4} (\text{°C}^{-1})$ . The resistance of the pressure sensor increased linearly as the ambient air pressure increased with its average sensitivity calculated as  $3.5 \times 10^{-2} (\Omega/\text{kPa})$ . The sensitivity of the humidity sensor increased with an increase in ambient temperature, due to the effect of temperature on its dielectric constant, which was determined to be 16.9, 21.4, 27.0, and 38.2 (pF/%RH) at 27°C, 30°C, 40°C, and 50°C, respectively. The rate of airflow was obtained by evaluating the sum of all variations between sensing resistors as the airflow passed over the flow sensor. The sensitivity to the rate of airflow was  $4.2 \times 10^{-2}$ ,  $9.2 \times 10^{-2}$ , and  $9.7 \times 10^{-2} (\Omega/\text{ms}^{-1})$  producing charges of 0.2, 0.3, and 0.5W, respectively.

## References

- [1] Chen, L.T.; Chang, J.S.; Hsu, C.Y.; Cheng, W.H. Fabrication and Performance of MEMS-Based Pressure Sensor Packages Using Patterned Ultra-Thick Photoresists. *Sensors* 2009, 9, 6200–6218.
- [2] Wang, Y.H.; Lee, C.Y.; Chiang, C.M. A MEMS-based Air Flow Sensor with a Free-standing Microcantilever Structure. *Sensors* 2007, 7, 2389–2401.
- [3] Ma, R.H.; Wang, D.A.; Hsueh, T.H.; Lee, C.Y. A MEMS-Based Flow Rate and Flow Direction Sensing Platform with Integrated Temperature Compensation Scheme. *Sensors* 2009, 9, 5460–5476.
- [4] Arshak, K.; Twomey, K. Thin films of In<sub>2</sub>O<sub>3</sub>/SiO<sub>2</sub> for Humidity Sensing Applications. *Sensors* 2002, 2, 205–218.
- [5] Arshak, K.; Twomey, K.; Egan, D. A Ceramic Thick Film Humidity Sensor Based on MnZn Ferrite. *Sensors* 2002, 2, 50–61.
- [6] Gogoi, B.P.; Mastrangelo, C.H. A Low Voltage Force-Balanced Barometric Pressure Sensor. In *Proceedings of International Electron Devices Meeting (IEDM)*, San Francisco, CA, USA, 8–11 December 1996; pp. 529–532.

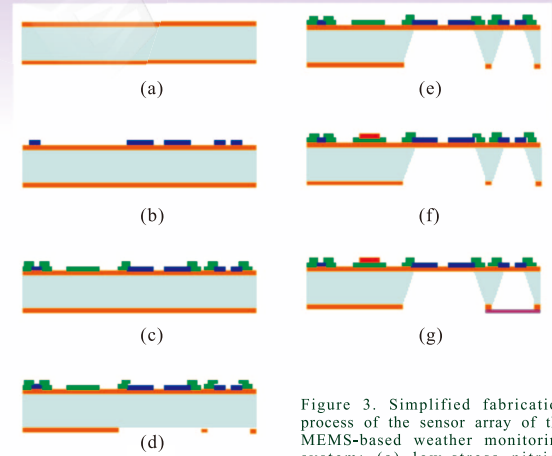


Figure 3. Simplified fabrication process of the sensor array of the MEMS-based weather monitoring system: (a) low-stress nitride deposition on silicon wafer, (b) electro-beam evaporation of Pt/Cr, (c) electro-beam evaporation of Au/Cr, (d) SF<sub>6</sub> RIE, (e) back-etching, (f) spin-on polyimide, (g) UV bonding and forming vacuum-sealed cavity at the pressure sensor.

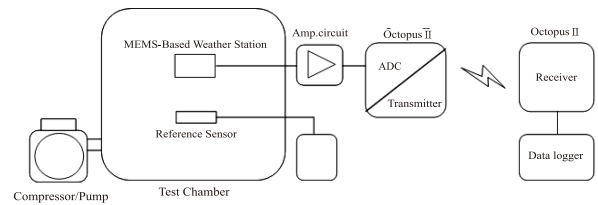


Figure 4. Schematic illustration of the wireless remote weather monitoring system for temperature, humidity and pressure.

Sensor	Amp. Circuit	$\mu$ -controller
Flow Sensor	$R_g$ $R_w$ $R_z$ $R_{rt}$ $R_{ze}$ $R_{rw}$ $R_{re}$ $R_{zw}$	$V_g$ $V_w$ $V_z$ $V_{rt}$ $V_{ze}$ $V_{rw}$ $V_{re}$ $V_{zw}$
Pressure Sensor	$R_{pres}$	$V_{pres}$
Temperature Sensor	$R_{temp}$	$V_{temp}$
Humidity Sensor	$C_{humi}$	$V_{humi}$

Figure 5. The signal determination path of the sensor array.

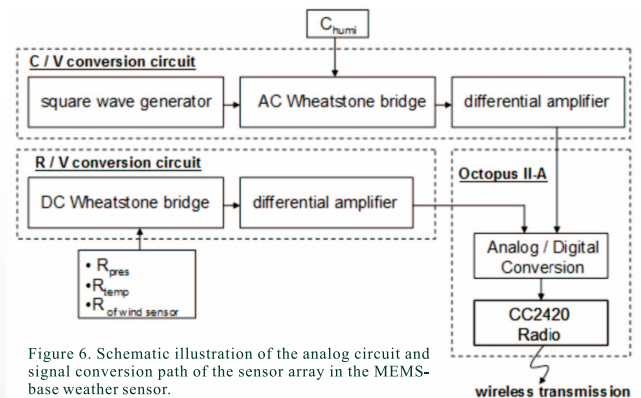


Figure 6. Schematic illustration of the analog circuit and signal conversion path of the sensor array in the MEMS-based weather sensor.

- [7] Mayer, F.; Haberli, A.; Jacobs, H.; Ofner, G.; Paul, O.; Balter, H. A Single Chip CMOS Anemometer. In *Proceedings of International Electron Devices Meeting (IEDM)*, Washington, DC, USA, 7–10 December 1997; pp. 895–898.
- [8] Rittersma, Z.M. Recent Achievement in Miniaturized Humidity Sensors—A Review of Transduction Techniques. *Sens. Actuata. A* 2002, 96, 196–210.
- [9] Lee, C.Y.; Lee, G.B. Humidity Sensors: A Review. *Sens. Lett.* 2005, 3, 1–14.
- [10] Bakker, A. CMOS Smart Temperature Sensor—An Overview. In *Proceedings of the IEEE Conference on Sensors*, Orlando, FL, USA, 12–14 June 2002; pp. 1423–1427.